ORIGINAL ARTICLE

Metastasis suppressor 1 controls osteoblast differentiation and bone homeostasis through regulating Src-Wnt/β-catenin signaling

Meng Chen[1] · Liying Shan[1] · Ying Gan[1] · Lijie Tian[1] · Jie Zhou[1] · Endong Zhu[1] · Hairui Yuan[1] · Xiaoxia Li[2] · Baoli Wang[1]

Abstract

Metastasis suppressor 1 (MTSS1) plays an inhibitory role in tumorigenesis and metastasis of a variety of cancers. To date, the function of MTSS1 in the differentiation of marrow stromal progenitor cells remains to be explored. In the current study, we investigated whether and how MTSS1 has a role in osteoblast differentiation and bone homeostasis. Our data showed that MTSS1 mRNA was upregulated during osteoblast differentiation and downregulated in the osteoblastic lineage cells of ovariectomized and aged mice. Functional studies revealed that MTSS1 promoted the osteogenic differentiation from marrow stromal progenitor cells. Mechanistic explorations uncovered that the inactivation of Src and afterward activation of canonical Wnt signaling were involved in osteoblast differentiation induced by MTSS1. The enhanced osteogenic differentiation induced by MTSS1 overexpression was attenuated when Src was simultaneously overexpressed, and conversely, the inhibition of osteogenic differentiation by MTSS1 siRNA was rescued when the Src inhibitor was supplemented to the culture. Finally, the in vivo transfection of MTSS1 siRNA to the marrow of mice significantly reduced the trabecular bone mass, along with the reduction of trabecular osteoblasts, the accumulation of marrow adipocytes, and the increase of phospho-Src-positive cells on the trabeculae. No change in the number of osteoclasts was observed. This study has unraveled that MTSS1 contributes to osteoblast differentiation and bone homeostasis through regulating Src-Wnt/β-catenin signaling. It also suggests the potential of MTSS1 as a new target for the treatment of osteoporosis.

Keywords Osteoblast · Differentiation · Metastasis suppressor 1 · Src · Wnt/β-catenin

Abbreviations

ALP	Alkaline phosphatase
BMP2	Bone morphogenetic protein 2
BMSCs	Bone marrow mesenchymal stem cells
C/EBP	CCAAT/enhancer binding protein
FBS	Fetal bovine serum
GSK3β	Glycogen synthase kinase 3β
HRP	Horseradish peroxidase
LRP6	Low-density lipoprotein receptor-related protein 6
MTSS1	Metastasis suppressor 1
OPN	Osteopontin
PPARγ	Peroxisome proliferator-activated receptor γ
QRT-PCR	Quantitative reverse transcription polymerase chain reaction
Runx2	Runt-related transcription factor 2
siRNA	Small interfering RNA
TCF7L2	Transcription factor 7-like 2
TRAP	Tartrate-resistant acid phosphatase

Meng Chen and Liying Shan contributed equally to the work.
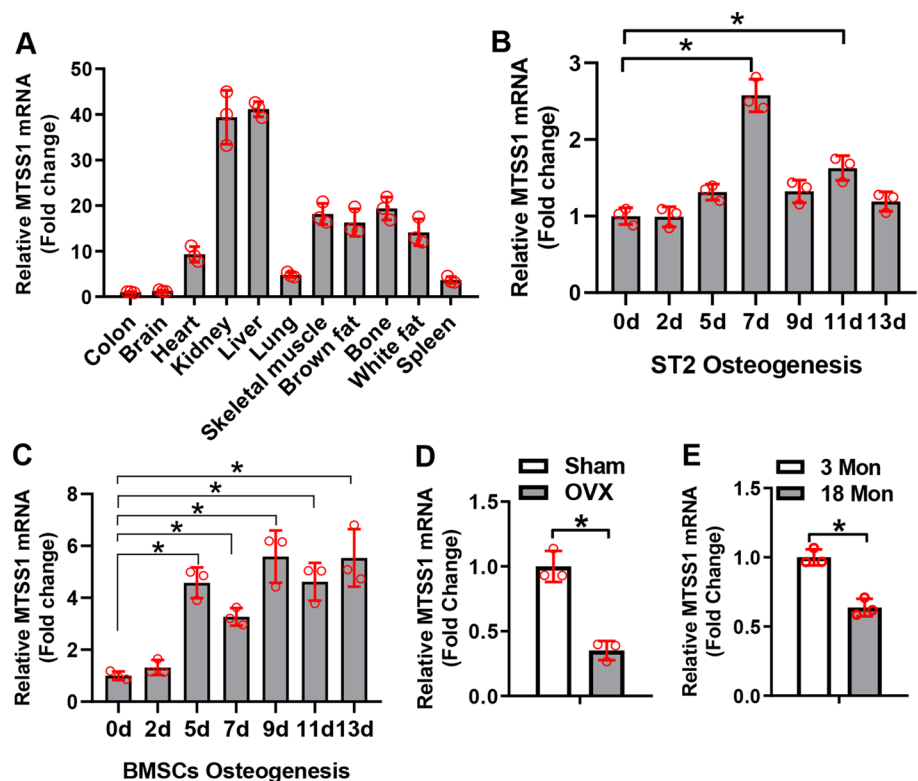
✉ Baoli Wang
blwang@tmu.edu.cn

[1] NHC Key Lab of Hormones and Development, Tianjin Key Lab of Metabolic Diseases, Chu Hsien-I Memorial Hospital & Institute of Endocrinology, Tianjin Medical University, 6 Huan-Rui-Bei Road, Tianjin 300134, China

[2] College of Basic Medical Sciences, Tianjin Medical University, Tianjin 300070, China

Introduction

Bone marrow mesenchymal stem cells (BMSCs) have the potential to differentiate toward multiple cell types, including osteoblasts, adipocytes, chondrocytes, and myoblasts. Under normal physiological conditions, the capabilities of BMSCs to differentiate toward osteoblastic and adipogenic

lineages are similar, and therefore, a reciprocal and competitive relationship usually exists between osteogenesis and adipogenesis [1, 2]. Certain pathological conditions might render BMSCs more committed toward one aspect of osteogenesis or adipogenesis at the expense of the other aspect, thereby lead to metabolic bone disorders, such as osteoporosis and osteopetrosis [1].

The modulation of osteogenic and adipogenic commitment of BMSCs is finely orchestrated by a variety of transcription factors and signaling pathways, including runt-related transcription factor 2 (Runx2), osterix, bone morphogenetic proteins (BMPs), and Wnt/β-catenin pathway, which usually positively control osteogenic differentiation [3–7]. In contrast, the transcription factors, i.e., peroxisome proliferator-activated receptor γ (PPARγ) and CCAAT/enhancer binding proteins (C/EBPs), are the major positive regulators of adipocyte differentiation [8, 9].

Metastasis suppressor 1 (MTSS1), also referred to as missing in metastasis (MIM), is a cytoskeletal scaffold protein which binds to actin and affects cytoskeleton organization [10]. MTSS1 is widely expressed in various tissues, e.g., spleen, thymus, testis, prostate, uterus, colon, and peripheral blood [11]. Accumulating evidences have established the inhibitory function of MTSS1 in tumorigenesis and metastasis of a variety of cancers, including the carcinomas of bladder [12, 13], stomach [14], breast [15], pancreas [16], colorectum [17], and lung [18]. Its low expression in these cancers is associated with poor prognosis. However, in the past few years, controversial findings arose which identified MTSS1 to be a metastasis driver in several types of tumors, such as melanoma [19] and hepatitis B-related hepatocellular carcinoma [20].

To date, the function of MTSS1 in the differentiation of marrow stromal progenitor cells is completely unknown. In the current study, we explored whether and how MTSS1 has a role in osteoblast differentiation and bone homeostasis. The data uncovered the pro-osteogenic function of MTSS1 in vitro and in vivo and elucidated the mechanism involved in the processes.

Results

MTSS1 was upregulated during osteoblast differentiation and downregulated in ovariectomized and aged mice

The expression level of MTSS1 was detected in various tissues of 6-week-old mice. Quantitative reverse transcription polymerase chain reaction (qRT-PCR) showed that MTSS1 mRNA was most abundant in liver and kidney, while it was moderately expressed in bone, skeletal muscle, and brown and white fat (Fig. 1A). The expression profiling of MTSS1 during osteogenic differentiation of progenitor cells was studied, which showed that MTSS1 was upregulated at day 7 and day 11 of ST2 differentiation (Fig. 1B), and upregulated

at day 5 through day 13 of BMSCs differentiation (Fig. 1C). Moreover, MTSS1 was significantly reduced in the BMSCs isolated from ovariectomized (OVX) mice *vs.* those from sham-operated mice (Fig. 1D). It was also decreased in the calvarial bone of 18-month-old aged mice *vs.* that of 3-month-old young mice (Fig. 1E). These results suggest that MTSS1 may have a role in osteogenic differentiation of stromal progenitor cells.

MTSS1 stimulated osteogenic differentiation of stromal progenitor cells

To elucidate the role of MTSS1 in osteogenesis, loss-of-function and gain-of-function experiments were performed. For the loss-of-function study, qRT-PCR and Western blotting analysis verified the efficacy of the MTSS1 shRNA lentivirus in silencing the endogenous expression of MTSS1 in primary BMSCs (Fig. 2A). Functionally, after osteogenic treatment, the knockdown of MTSS1 in primary BMSCs suppressed osteogenic differentiation, which was evidenced by the attenuation of alkaline phosphatase (ALP) staining and alizarin red staining (Fig. 2B). Accordingly, the mRNA and/or protein expression levels of the osteogenic factors, such as Runx2, osterix, ALP, and osteopontin, were reduced in the cells underexpressing MTSS1 as compared to those infected with control virus (mRNAs reduced by 30~87% and proteins reduced by 60~88%) (Fig. 2C, D). Moreover, MTSS1 silencing in ST2 cells following the transfection of MTSS1 small interfering RNAs (siRNAs) also attenuated the osteogenic differentiation as compared to the control cells (Fig. 2E–H). Furthermore, MTSS1 silencing did not significantly change the cell growth rate of ST2 cells (Fig. 2I).

For the gain-of-function study, qRT-PCR analysis verified the overexpression of MTSS1 in ST2 following the transfection of the MTSS1 expression construct (Fig. 3A). Functionally, after osteogenic treatment, the overexpression of MTSS1 in ST2 cells stimulated osteogenic differentiation, which was evidenced by the enhancement of ALP staining (Fig. 3B). Accordingly, the mRNA and/or protein expression levels of the osteogenic factors were increased in the cells overexpressing MTSS1 as compared to those transfected with the vector (mRNAs increased by 1.55~3.29-fold and proteins increased by 42~68%) (Fig. 3C, D). Furthermore, MTSS1 overexpression did not significantly change the cell growth rate of ST2 cells (Fig. 3E).

MTSS1 inactivated Src and activated Wnt/β-catenin signaling in stromal progenitor cells

We then tried to uncover the mechanism by which MTSS1 regulates osteoblast differentiation. The data showed that the dysregulation of MTSS1 altered Src signaling. Briefly,

Western blotting analysis revealed that MTSS1 overexpression inhibited, while MTSS1 depletion stimulated the phosphorylation of Src (Y419) in ST2 cells (Fig. 4A, B). The results from Co-IP experiment revealed that Src physically interacted with MTSS1 and low-density lipoprotein receptor-related protein 6 (LRP6) (Fig. 4C). Moreover, Western blotting analysis showed that the overexpression of MTSS1 significantly increased, while its knockdown decreased the protein levels of phosphorylated LRP6 (S1490), phosphorylated glycogen synthase kinase 3β (GSK3β) (S9), non-phospho-β-catenin, and transcription factor 7-like 2 (TCF7L2) (Fig. 4D, E). Consistently, the overexpression of Src significantly decreased phosphorylated GSK3β (S9), non-phospho-β-catenin, and TCF7L2 (Fig. 4F).

Dysregulation of Src expression impaired osteogenic differentiation of progenitor cells

To further elucidate the involvement of Src in MTSS1-regulated osteogenesis, Src gain-of-function experiment was performed. qRT-PCR and Western blotting analysis verified the efficacy of the Src expression construct in supplementing the level of Src in ST2 cells (Fig. 5A). Functionally, after osteogenic treatment, the overexpression of Src in ST2 cells suppressed osteogenic differentiation, as evidenced by the attenuation of ALP staining (Fig. 5B). Accordingly, the mRNA and/or protein levels of the osteogenic factors were reduced in the cells overexpressing Src as compared to those transfected with vector (mRNAs reduced by 46~56% and proteins reduced by 50~61%) (Fig. 5C, D). Furthermore, Src mRNA was elevated in the BMSCs of ovariectomized mice (Fig. 5E).

Moreover, we performed cotransfection experiment to investigate if Src is able to relieve the disturbed osteogenesis induced by MTSS1. The results showed that under osteogenic condition, the cells cotransfected with MTSS1 expression construct and vector displayed enhanced ALP staining and increased levels of osteogenic factors as compared to the cells transfected with vector only. This stimulatory effect of MTSS1 on osteogenesis was attenuated when the cells were cotransfected with MTSS1 and Src expression constructs (Fig. 6A–C). Conversely, the cells receiving MTSS1 siRNA and vehicle displayed repressed ALP staining and decreased levels of osteogenic factors as compared to the cells receiving control siRNA and vehicle. This anti-osteogenic effect of MTSS1 siRNA was attenuated when the cells received MTSS1 siRNA and Src inhibitor 1 (Src-I1) (Fig. 6D–E).

Fig. 2 Silencing of MTSS1 inhibited osteogenic differentiation of stromal progenitor cells. The knockdown of MTSS1 was verified using qRT-PCR in primary BMSCs isolated from 6-week-old mice (**A**) and ST2 cells (**E**) after infection of MTSS1 shRNA expression lentivirus or transfection of MTSS1 siRNAs. BMSCs or ST2 cells underexpressing MTSS1 were induced to allow osteogenic differentiation. The effects of MTSS1 silencing (BMSCs: **B–D**; ST2: **F–H**) on osteoblast differentiation were examined. Alizarin red staining and/or ALP staining were performed in differentiated osteoblasts 14 days and 21 days, respectively, after osteogenic treatment (**B**, **F**). The mRNA (**C**, **G**) and protein (**D**, **H**) levels of osteogenic factors were measured 72 h after osteogenic treatment. The effect of MTSS1 silencing on cell growth rate of ST2 cells was measured using a CCK-8 kit (**I**). Values represent mean ± SD, $n = 3$ in (**A**, **C**–**E**, **G**, **H**); n=8 in (**I**). Student's t test was conducted in (**A**, **C**, **D**). One-way ANOVA was conducted in (**E**, **G**, **H**, **I**) followed by Tukey test for post hoc comparisons. *Significant *vs.* control LV or control siRNA, $p < 0.05$
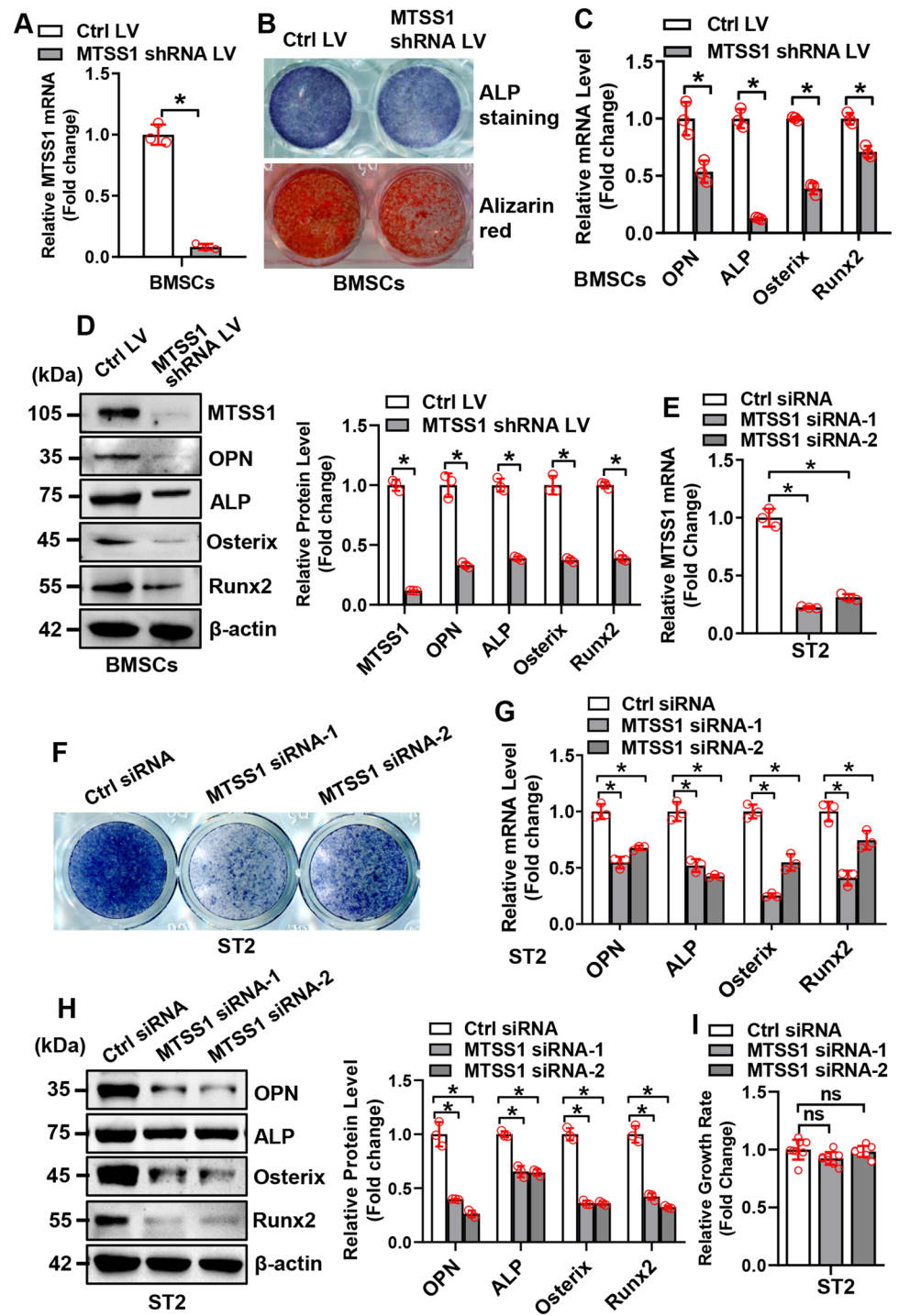


Silencing of MTSS1 impaired the differentiation of osteoblasts and reduced trabecular bone mass in mice

We further investigated the physiological role of MTSS1 in the differentiation of BMSCs in mice. qRT-PCR analysis demonstrated that the in vivo transfection of MTSS1 siRNA is effective in knocking down the endogenous expression of

MTSS1 in the BMSCs of the tibiae (Fig. 7A, B). Histomorphometric analysis using μCT showed that 4 weeks after the in vivo transfection, bone volume per tissue volume (BV/TV), bone mineral content per tissue volume (BMC/TV), and trabecular thickness (Tb.Th) were significantly decreased by 25%, 23% and 17%, respectively, in the mice receiving MTSS1 siRNA *vs.* those receiving control siRNA
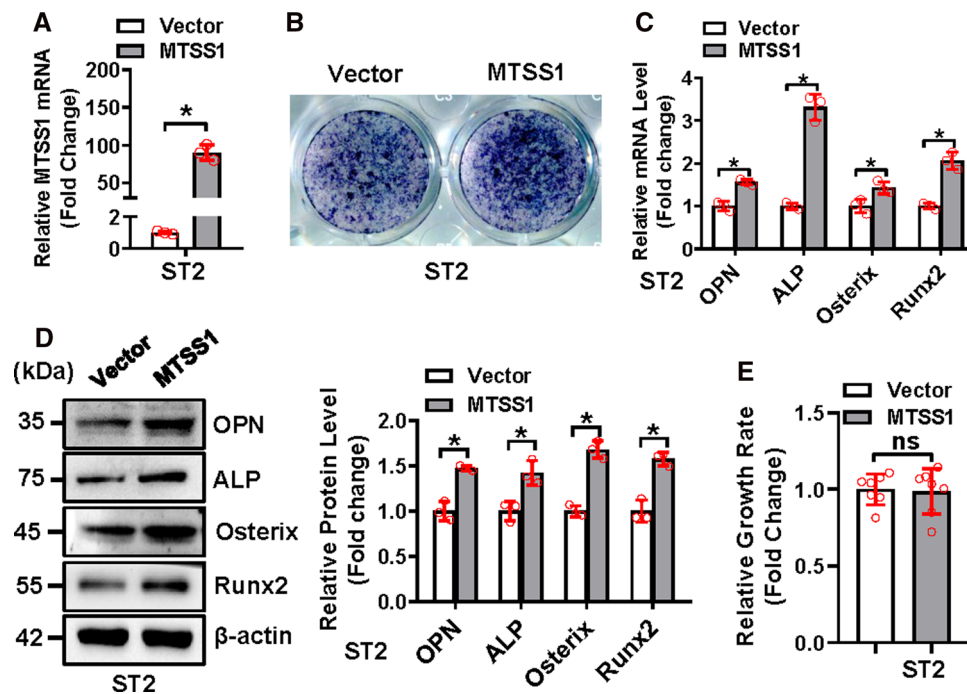
Fig. 3 Overexpression of MTSS1 stimulated osteogenic differentiation of stromal progenitor cells. The overexpression of MTSS1 was verified using qRT-PCR in ST2 cells after transfection of MTSS1 expression construct (A). The ST2 cells after transfection were induced to allow osteogenic differentiation. The effect of MTSS1 overexpression on osteoblast differentiation was examined. ALP staining was performed in differentiated osteoblasts 14 days after osteogenic treatment (B). The mRNA (C) and protein (D) levels of osteogenic factors were measured 72 h after osteogenic treatment. The effect of MTSS1 overexpression on cell growth rate of ST2 cells was measured using a CCK-8 kit (E). Values represent mean ± SD, $n = 3$ in (A, C, D); $n = 7$ in (E). Student's t test was conducted. *Significant $vs.$ vector, $p < 0.05$

(Fig. 7C–F). By contrast, the trabecular number (Tb.N) was not changed in the transfected mice (Fig. 7G).

We quantified the number of adipocytes, osteoblasts, and osteoclasts on the sections. H&E staining analysis showed that both the number and area of the adipocytes were increased in the mice receiving MTSS1 siRNA as compared to those receiving control siRNA (Fig. 8A–C). Immunohistochemical staining analysis showed that the ALP-positive osteoblasts were reduced in the mice receiving MTSS1 siRNA $vs.$ those receiving control siRNA (Fig. 8D, E). Moreover, the immunohistochemical staining analysis also showed that the mice receiving MTSS1 siRNA had more phospho-Src-positive cells on the trabeculae than the control mice (Fig. 8F, G). By contrast, tartrate-resistant acid phosphatase (TRAP) staining analysis did not reveal any change in the number of osteoclasts (Fig. 8H, I). Furthermore, qRT-PCR analysis revealed that the overexpression of MTSS1 in ST2 cells did not change the ratio of RANKL to OPG (Fig. 8J).

Discussion

Previously, the research interests in MTSS1 were mainly focused on its function in tumorigenesis and metastasis of various cancers. In this study we aimed to find some novel function of MTSS1 in bone. Based on the observation that MTSS1 was upregulated during osteoblast differentiation and downregulated in the osteoblastic lineage cells from the ovariectomized mice and aged mice, we hypothesized that MTSS1 may have a regulatory role in osteogenesis and bone homeostasis.

To delineate the exact role of MTSS1 in osteogenesis, loss-of-function and gain-of-function experiments were applied using primary BMSCs and/or stromal cell line. It appeared that MTSS1 did not affect the cell growth rate of the progenitor cells. However, it was shown that the overexpression of MTSS1 stimulated, while the depletion of MTSS1 inhibited the differentiation of osteoblasts and the expression of the osteogenic transcription factors and marker genes. Of more importance, in vivo experiments showed that the depletion of MTSS1 in the marrow resulted in the reduction of trabecular osteoblasts and the accumulation

Fig. 4 MTSS1 inactivated Src and activated Wnt/β-catenin signaling in stromal progenitor cells. ST2 cells were transfected with MTSS1 expression construct (**A**, **D**) or MTSS1 siRNA (**B**, **E**) or Src expression construct (**F**) and their control. The protein levels of MTSS1, phosphorylated, and total Src were detected in the cells 3 days after transfection using Western blotting (**A**, **B**). Co-IP was performed between endogenous MTSS1 and LRP6 were detected with Western blotting (**C**). The protein levels of the major components of Wnt/β-catenin signaling were detected in the cells 3 days after transfection using Western blotting (**D–F**). Values represent mean ± SD, $n = 3$. Student's t test was conducted in (**A**, **D**, **F**). One-way ANOVA was conducted in (**B**, **E**) followed by Tukey test for post hoc comparisons. *Significant *vs.* vector or control siRNA, $p < 0.05$
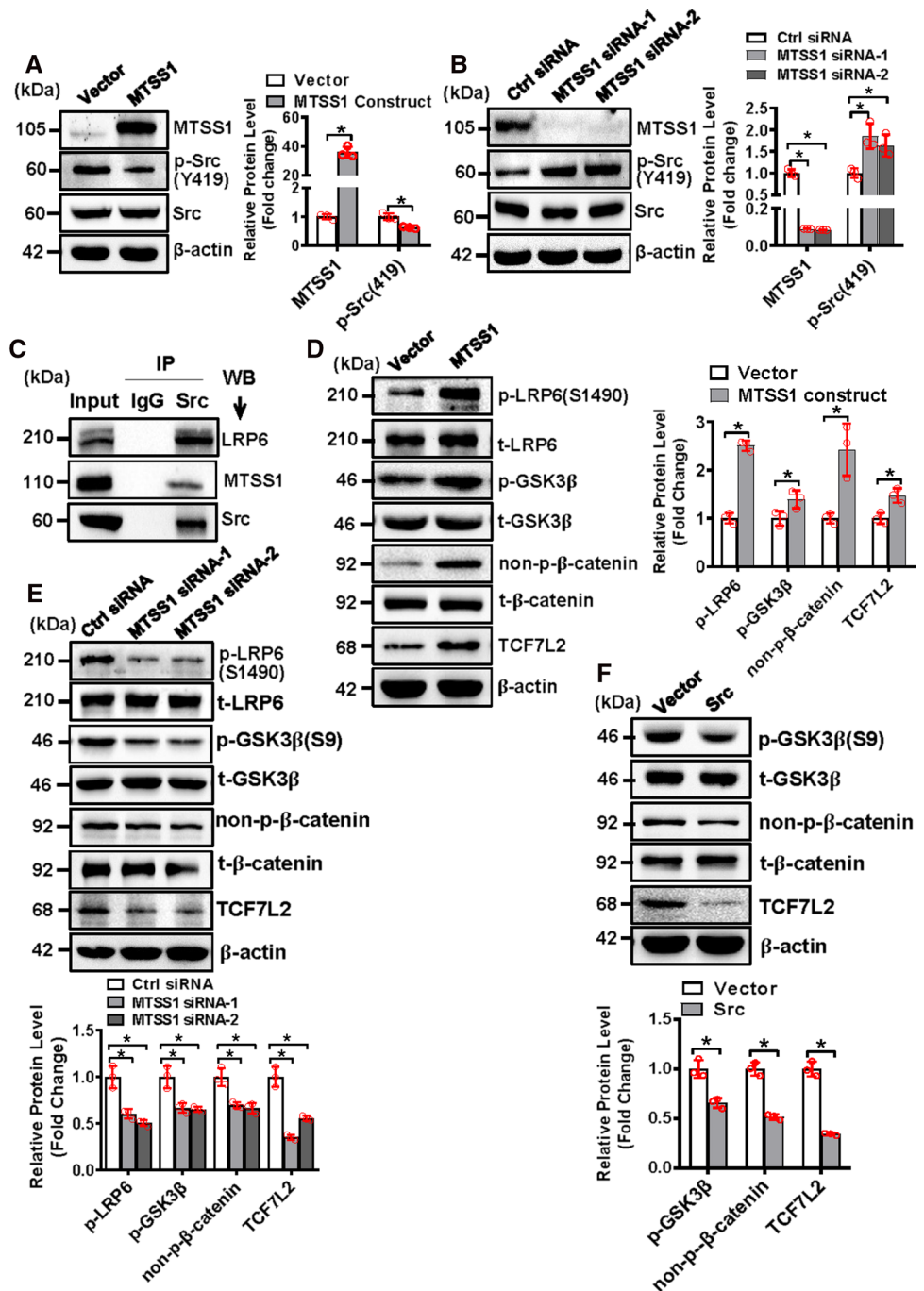
of marrow fat. Additionally, the trabecular bone mass was reduced in the mice following the knockdown of MTSS1 in the marrow, as indicated by the decline of trabecular bone volume and bone mineral content. Of note, it appears that the reduction of bone mass was mainly due to the reduction in the thickness of the trabeculae, while the number of trabeculae was not affected. Based on the observation that osteoclast number was similar between the two groups of mice, we

concluded that the reduction of trabecular bone mass is a result of the impaired formation of mature osteoblasts.

Of interest, Saarikangas et al. previously reported that MTSS1 was necessary for the maintenance of intercellular junctions in kidney epithelia and loss of MTSS1 resulted in a progressive kidney defect in mice. In addition, lower bone content was observed in the mutant mice, which was assumed to be a secondary effect of the kidney defect [21]. Based upon the function of MTSS1 we observed in
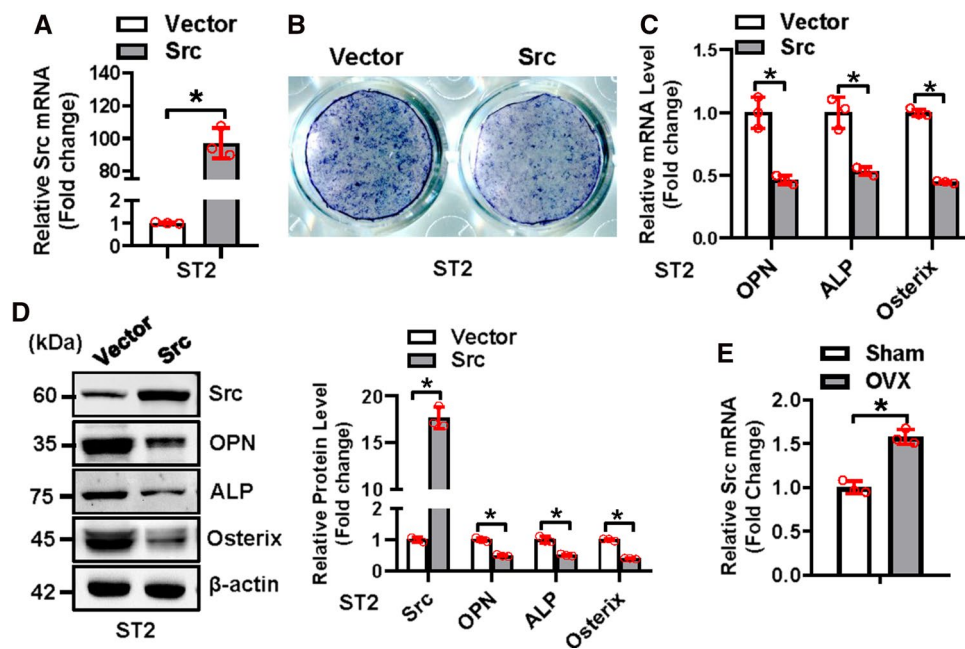
Fig. 5 Overexpression of Src impaired osteogenic differentiation of progenitor cells. The overexpression of Src was verified using qRT-PCR in ST2 cells after transfection of Src expression construct (**A**). The ST2 cells after transfection were induced to allow osteogenic differentiation. The effect of Src overexpression on osteoblast differentiation was examined. ALP staining was performed in differentiated osteoblasts 14 days after osteogenic treatment (**B**). The mRNA (**C**) and protein (**D**) levels of osteogenic factors were measured 72 h after osteogenic treatment. Src mRNA level was examined using qRT-PCR in the BMSCs of 16 week-old mice 8 weeks after ovariectomy (**E**). Values represent mean ± SD, $n = 3$. Student's t test was conducted. *Significant *vs.* vector, $p < 0.05$
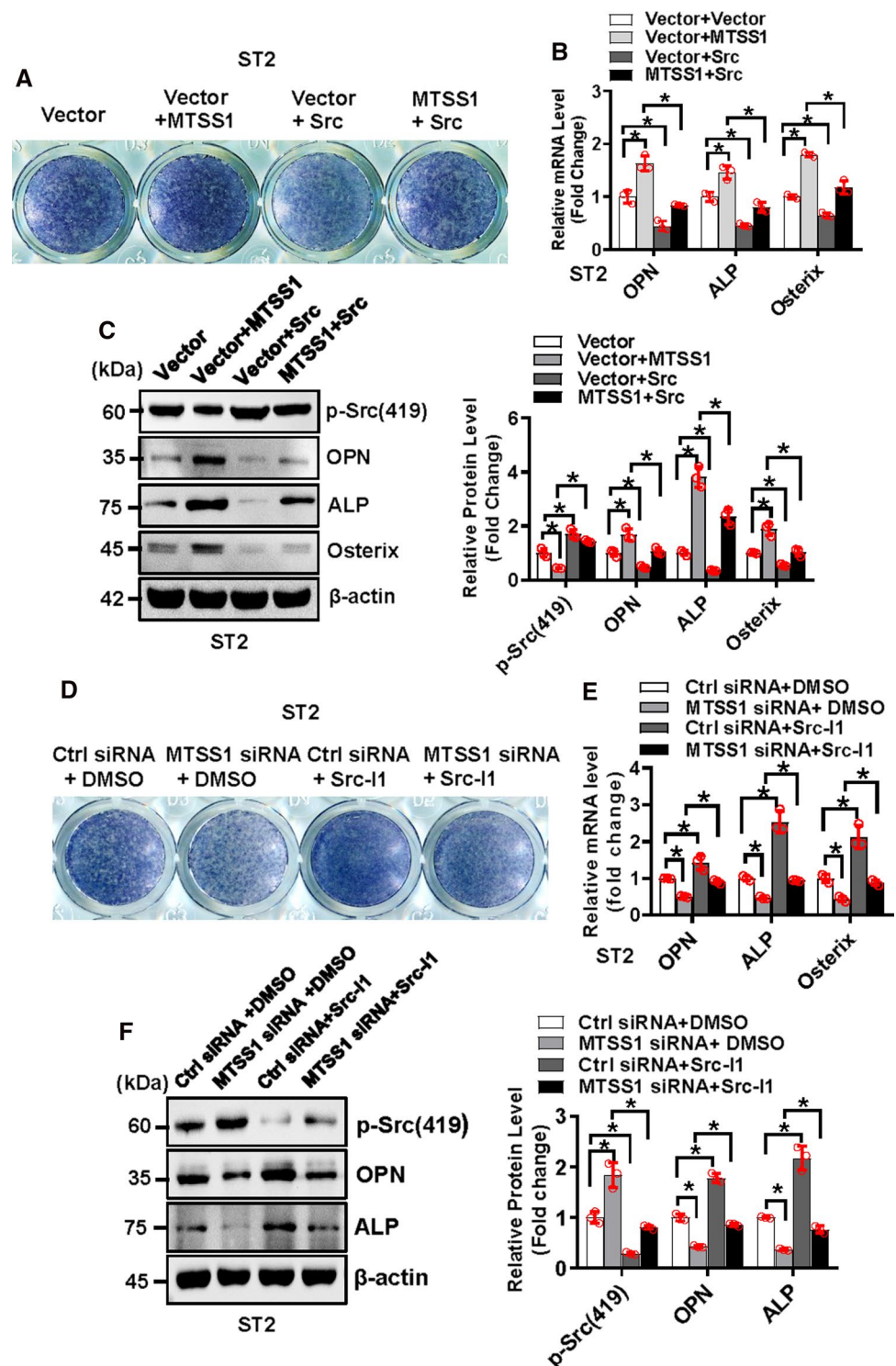
regulating osteoblast differentiation and bone homeostasis, we propose that the lower bone mass observed in the MTSS1 null mice may also be due to the defect of osteoblast differentiation.

MTSS1 is one of the defining members of the I-BAR family of negative membrane curvature-sensing proteins that was initially identified to be absent in metastatic bladder cancer [11]. It contains a C-terminal WH2 actin-binding motif and functions as a cytoskeletal remodeling protein [10]. MTSS1 is now considered to be the antagonist of Src family of tyrosine kinases (SFK) in a variety of cellular activities. Quinones et al. provided the first genetic evidence that MTSS1 modulated directed cell migration by suppressing endocytosis and the activities of the CD2-associated protein/cortactin complex [22]. Another group reported that the MTSS1-dependent antagonism of cortactin in promoting ciliogenesis was mediated by the SFK [23]. Consistently, MTSS1 loss in mice resulted in increased SFK activity in Purkinje neurons, degenerating Purkinje neurons with low firing rates, and cell death [24]. In our study, we demonstrated that MTSS1 directly interacted with Src. Of interest, we also observed the hypo-phosphorylation of Src following the overexpression of MTSS1 and hyper-phosphorylation of Src after the knockdown of MTSS1 in stromal progenitor cells. These data suggest that Src acts in response to MTSS1

to mediate the regulatory function of the latter in stromal progenitor cells.

The proto-oncogene Src has long been studied about its role in bone homeostasis. Based on the evidences from genetic animal models, Src is detrimental to bone mass accrual because Src null mice displayed severe osteopetrosis [25]. The cellular basis for the phenotype involved the impairment in both osteoclasts and osteoblasts. Src is critical for the normal cytoskeletal architecture of osteoclasts [26]. Src null mice had more osteoclasts which did not form ruffled borders, thus functioned inappropriately and failed to resorb bone [27]. Moreover, the deletion of Src enhanced osteoblast differentiation and bone formation, contributing to the increase of bone mass as well [28]. In our study, we investigated the role of Src in vitro. It was shown that Src was able to suppress the differentiation of osteoblasts. Additionally, overexpression of Src in the progenitor cells attenuated the stimulation of osteoblast differentiation induced by MTSS1, and inhibition of Src activity in the progenitor cells attenuated the blockade of osteoblast differentiation induced by MTSS1 siRNA. These evidences further support the interaction of MTSS1 with Src in regulating osteogenic commitment. Of more interest, the mice receiving MTSS1 siRNA exhibited more phospho-Src in the trabecular bone cells, indicating the involvement of Src in the reduction of

Fig. 6 Src relieved the stimulation of osteogenic differentiation induced by MTSS1. ST2 cells were cotransfected with MTSS1 and Src expression construct or the vector, and were induced to allow osteogenic differentiation (**A–C**). Alongside, ST2 cells were transfected with control or MTSS1 siRNA, then induced to allow osteogenic differentiation in the osteogenic medium supplemented with 10 μm Src inhibitor 1 (Src-I1) (**D–F**). ALP staining was performed in differentiated osteoblasts 14 days after osteogenic treatment (**A**, **D**). The mRNA (**B**, **E**) and protein (**C**, **F**) levels of osteogenic factors were measured 72 h after osteogenic treatment. Values represent mean $\pm$ SD, $n = 3$. Two-way ANOVA was conducted followed by Tukey test for post hoc comparisons. $*p < 0.05$


bone mass observed in the mice transfected with MTSS1 siRNA.

Canonical Wnt signaling is one of the best characterized pathways that plays a key stimulatory role in osteoblast differentiation and bone formation [7]. It has been documented that Src interacts with canonical Wnt signaling, exhibiting either stimulatory or inhibitory effect on the latter depending on cellular context. In cancer cells, Src contributes to tumor progression at least partially through enhancing canonical Wnt signaling [29, 30]. Src acted as a positive regulator of β-catenin, which functioned by docking to and being activated by Dishevelled-2 in response

Fig. 7 Silencing of MTSS1 reduced trabecular bone mass in mice. qRT-PCR (**A**) and Western blotting (**B**) were done to verify the silencing of MTSS1 mRNA in the BMSCs isolated 48 h after in vivo transfection of MTSS1 siRNA. Three-dimensional reconstruction of µCT images are shown (**C**) and histomorphometric parameters were measured (**D–G**) in the mice 4 weeks after in vivo transfection. Data are mean ± SD. A: $n = 3$; **D–G**, n = 6. Student's t test was conducted. *$p < 0.05$ *vs.* Control siRNA
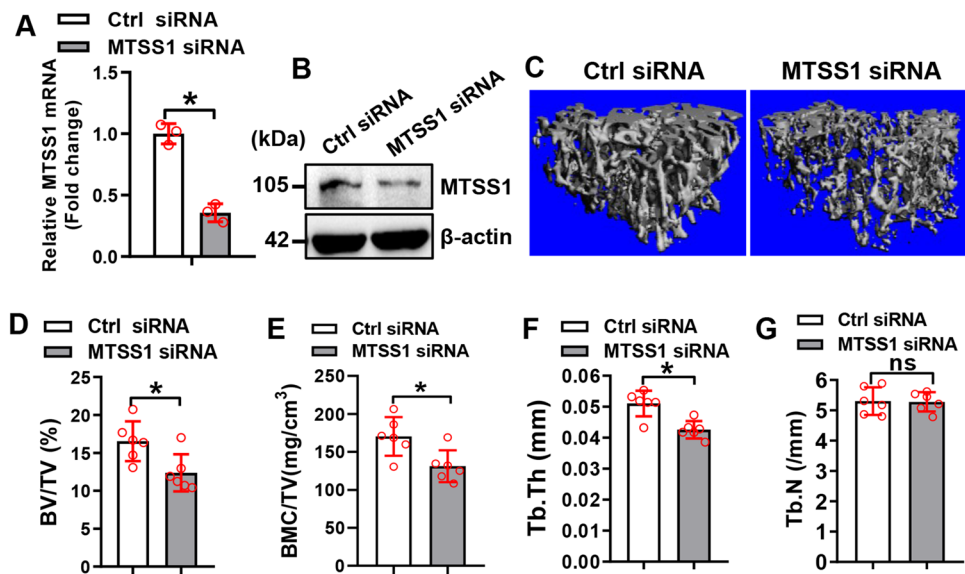

Fig. 8 Silencing of MTSS1 impaired the differentiation of osteoblasts in mice. Histological, histomorphometric, and immunohistochemical analyses were performed on the bone sections from the mice 4 weeks after transfection. H&E staining was done. Image scale: 500 µm (**A**). Numbers (**B**) and areas (**C**) of adipocytes were quantified. Representative images of immunohistochemical staining for ALP (**D**) and phospho-Src (**F**) are shown. Image scale: 20 µm (**D**, **F**). Numbers of ALP-positive osteoblasts (**E**) and phospho-Src-positive cells on the trabeculae were counted (**G**). Representative images of TRAP staining are shown. Image scale: 20 µm (**H**). Numbers of osteoclasts were counted (**I**). The mRNA expression of RANKL and OPG was detected in ST2 cells following MTSS1 overexpression and the ratio was calculated (**J**). Data are mean ± SD. Student's t test was conducted. $n = 6$ in (**B, C, E, G, I**), *$p < 0.05$ *vs.* Control siRNA. $n = 3$ in (**J**), *$p < 0.05$ *vs.* Vector
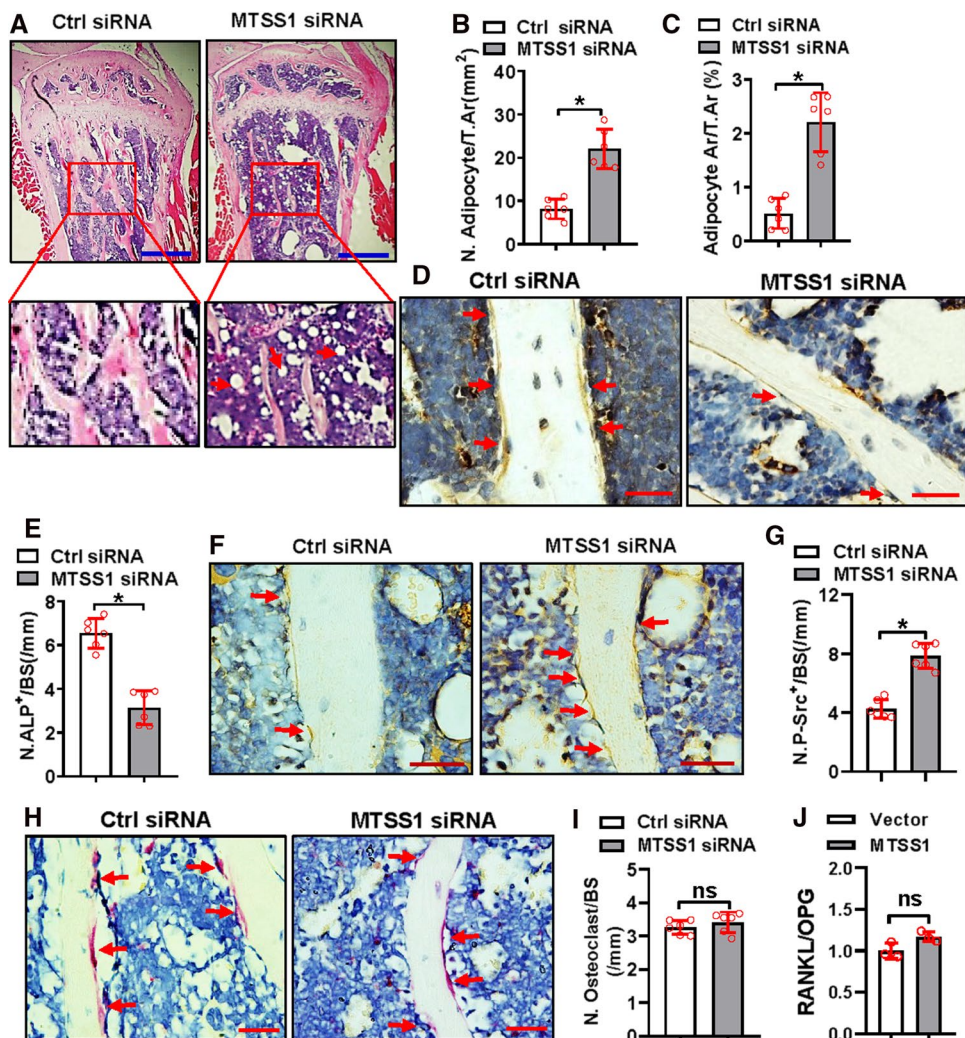
to Wnt stimulation [31]. Activated Src downregulated E-cadherin or phosphorylated β-catenin at Tyr(654), as a result facilitating the release of β-catenin from cadherin complex at the membrane and promoting accumulation of β-catenin in the nucleus, thus rendering it available for transcriptional regulation [32, 33]. Of interest, Chen et al. recently reported that in non-cancer cells, such as mouse embryonic fibroblasts (MEF), Src was both sufficient and necessary for suppressing canonical Wnt pathway [34]. Src associated with LRP6 directly phosphorylated LRP6 at several conserved tyrosine residues, leading to the removal of LRP6 from cell surface and the disruption of LRP6 signalosome formation, which eventually blocked the signal transduction of canonical Wnt signaling [34]. This appears to account for the fact that Src and canonical Wnt signaling have opposite effects on osteoblastogenesis and bone formation.

In this study, the Co-IP experiment demonstrated the physical binding of Src to LRP6, suggesting that Src might directly phosphorylate LRP6 in osteoblastic cell lineage. Furthermore, MTSS1 increased, while Src decreased the level of phospho-GSK3β (S9), non-phospho-β-catenin, and TCF7L2. Collectively, our data provide evidences that, consistent to Chen et al.'s report, Src in osteoblastic lineage also suppressed the activation of Wnt/β-catenin signaling, and that MTSS1 stimulated Wnt/β-catenin pathway through antagonizing the non-receptor tyrosine kinase Src.
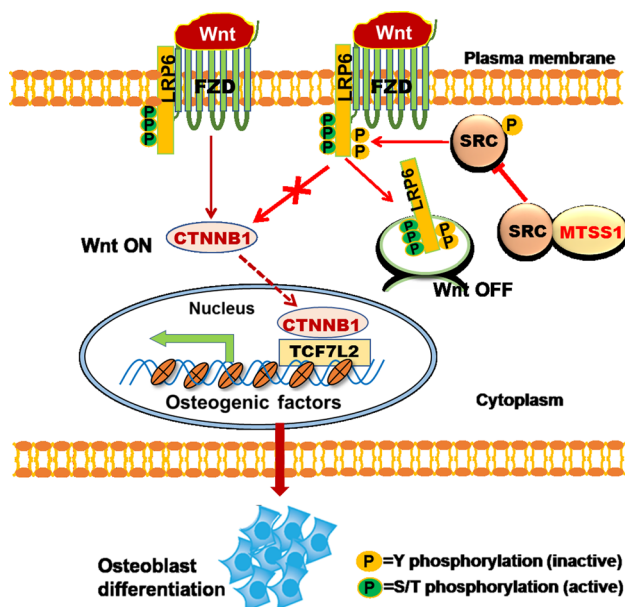
Fig. 9 Schematic diagram depicting the mechanism for MTSS1 in regulating osteoblast differentiation

Conclusion

In summary, we have identified a new osteogenic factor, MTSS1, which positively regulates the osteogenic differentiation of marrow stromal progenitor cells in vitro and in vivo, and contributes to the homeostasis of bone. Mechanistic investigations have revealed that the inactivation of Src and activation of Wnt/β-catenin signaling mediates the function of MTSS1 in the cell fate determination of bone marrow stromal progenitor cells and the homeostasis of bone (Fig. 9). Taken as a whole, the current study suggests that MTSS1 is a novel target for the therapeutic intervention of metabolic bone disorders, such as osteoporosis.

Materials and methods

Cells

ST2 cells were maintained in α-MEM supplemented with 10% fetal bovine serum (FBS). Primary murine BMSCs were collected from the femurs and tibiae of mice. Briefly, the bone marrow was flushed from 6-week-old C57BL/6 mice with α-MEM using a 26-gauge syringe and the marrow cells were seeded in a 10 cm dish at the density of $3 \times 10^5/cm^2$ in α-MEM supplemented with 20% FBS. After culturing for 3 days, the non-adherent hematopoietic cells were removed by changing the culture medium with α-MEM containing 10% FBS. The medium was refreshed every 3 days. At 70–80% confluence, the cells were trypsinized by 0.25% trypsin/EDTA and passaged. The cells at passage 3–5 were induced to allow differentiation using osteogenic medium containing 50 μg/mL ascorbic acid and 10 mM β-glycerophosphate. After 3 days of induction, the cells underwent RNA and protein extraction and after 14 days or 21 days of induction, the cells underwent ALP staining or alizarin red staining to evaluate the status of differentiation.

siRNAs, construct, and transfections

For the gain-of-function studies, the gene sequence coding for full-length Src was PCR amplified, then cloned into the eukaryotic expression vector pcDNA3.1(+) at the sites of BamHI/EcoRI using the ClonExpress II One Step Cloning Kit (Vazyme, Nanjing, China). The expression construct of MTSS1 was purchased from Origene (Rockville, MD, USA). Each construct or the vector was transfected into ST2 cells at the confluence of 70–80% using JetPRIME transfection reagent (Polyplus, Illkirch, France). For the cotransfection experiment, the expression construct of MTSS1 or the vector was cotransfected with Src expression construct or the vector into ST2 cells using JetPRIME transfection reagent. After

4 h of transfection, the transfection medium was removed and replaced with complete culture medium. The cells were induced at appropriate confluence to allow osteogenic differentiation.

For the loss-of-function studies, the siRNAs specifically targeting the coding sequence of MTSS1 or Src were designed and synthesized (Genepharma, Shanghai, China). Each target or control siRNA, at the concentration of 20 nmol/L, was transfected into ST2 cells at 50–60% confluence using lipofectamine RNAi-max reagent (Invitrogen, Carlsbad, CA, USA). After 24 h of transfection, the transfection medium was replaced with complete culture medium. The cells were induced at appropriate confluence to allow osteogenic differentiation.

The sequences of the primers and siRNAs are listed in Supplemental Tables S1 and S2, respectively.

Cell proliferation assay

The cells were grown in a 96-well plate, transfected with the construct overexpressing MTSS1 (or vector) or the siRNAs silencing MTSS1 (or control siRNA) following the protocols as mentioned above. 24 h after transfection, CCK-8 solution was added and the effect of MTSS1 was assessed by using a CCK-8 cell counting kit (Vazyme, Nanjing, China).

qRT-PCR

Total RNA was extracted from tissues using RNAiso Plus (Takara, Dalian, China), or from cells using a RNA extraction kit (Omega, USA) following the supplier's instructions. 0.5 μg RNA was reverse transcribed using the MMLV reverse transcriptase (Thermo Fisher, Waltham, MA, USA) in the presence of oligo(dT) and random primer. The resulting cDNAs were used as templates for quantitative PCR using the SYBR-Green Master PCR Mix (Abclonal, Wuhan, China). The relative expression level of each target gene was calculated following the comparative $\Delta\Delta Ct$ method with β-actin as the internal control for normalization. The primers for the PCR reactions are listed in Supplemental Table S1.

Western blot analysis

Cells were harvested in RIPA lysis buffer and protein contents of the cell lysates were quantified by a BCA Assay kit (Beyotime, Shanghai, China). Proteins were separated on 10–15% sodium dodecyl sulfate–polyacrylamide gel electrophoresis (SDS-PAGE) and transferred onto nitrocellulose membranes. After blocking with 5% skim milk, the membranes were probed with primary antibodies at 4 °C overnight, then incubated with horseradish peroxidase (HRP)-conjugated secondary antibodies. The immunoreactive bands were detected using a chemiluminescence reagent (Proteintech, Wuhan, China). β-actin was used as a loading control and the relative protein expression level of each target gene was calculated by dividing the optical density of the target gene with that of β-actin. The primary antibodies used are as follows: antibodies from Abcam (Cambridge, MA, USA): anti-TCF7L2 (ab76151), anti-LRP6 (ab134146), anti-osterix (ab94744), and anti-ALP (ab108337); antibodies from Cell Signaling Technology (Danvers, MA, USA): anti-Runx2 (#12556), anti-non-phospho-β-catenin (#8814), anti-phospho-LRP6 (S1490) (#2568), anti-GSK3β (#12456), and anti-phospho-GSK3β (S9) (#5558); antibodies from Abclonal (Wuhan, China): anti-MTSS1 (A11697), and anti-Src (A19119); antibody from Affinity (Changzhou, China): anti-Phospho-Src (Y419) (AF3162); and antibodies from Proteintech (Wuhan, China): anti-β-catenin (51067–2-AP), anti-osteopontin (25715–1-AP), and anti-β-actin (66009–1-Ig).

Lentiviral packaging and infection

To carry out loss-of-function experiment in primary BMSCs, a pair of oligos coding for the shRNA of MTSS1 was annealed, then ligated to pLVX-shRNA2 vector at BamHI/EcoRI sites (Clontech, Mountain View, CA, USA). The lentiviruses were packaged using a kit from Jiman Biotech (Shanghai, China) following the supplier's instructions. Briefly, the lentiviral shRNA expression construct or the vector was transfected, respectively, into 293 T cells together with the packaging plasmids. 48 h after transfection, the supernatant containing the viruses was collected, purified, and titered. The primary BMSCs were infected with the virus with a multiplicity of infection (MOI) of 20, then induced with osteogenic medium at 70–80% confluence to allow differentiation.

Alkaline phosphatase (ALP) staining and alizarin red staining

After 14 days of osteogenic treatment, the differentiated osteoblasts underwent ALP staining. Briefly, the cell cultures were rinsed with PBS, fixed for 10 min with 4% paraformaldehyde, and then stained for 20 min with NBT/BCIP staining solution (Beyotime, Shanghai, China). The differentiated osteoblasts underwent alizarin red staining after 21 days of osteogenic treatment. Briefly, the cultures were fixed for 10 min with 4% paraformaldehyde, then stained for 5 min with 1% alizarin red stain solution (pH 4.2).

Co-immunoprecipitation (Co-IP)

The cells were washed with ice-cold phosphate buffered saline (PBS) and lysed with RIPA buffer supplemented with protease inhibitors. After lysis, 500 μg of each protein sample was incubated at 4 °C with the primary antibody against Src or rabbit IgG. To capture the immunocomplexes, protein A/G magnetic beads were added and incubated for 2 h at 4 °C. The supernatant was discarded and the beads were washed with PBS plus 0.5% Triton X100, and then boiled in SDS sample buffer. The denatured samples were then subjected to SDS-PAGE and immunoblot analysis for MTSS1 and LRP6.

In vivo delivery of siRNAs

C57BL/6 mice were obtained from SPF Biotechnology (Beijing, China) and housed in SPF facility. The mice had free access to food and water and were kept with a controlled 12 h light:12 h dark cycle. To deliver the siRNAs to the bone marrow of mice, 2′-Ome-modified MTSS1 siRNA or control siRNA (Genepharma, Shanghai, China) was formulated with in vivo-JetPEI (Polyplus, Illkirch, France) following the supplier's instructions. Briefly, for one mouse, 11 μg siRNA and 1.5 μL in vivo-JetPEI were diluted, respectively, with 12.5 μl of 5% glucose and then mixed. Afterward, the formulated mixture was injected to the marrow cavity of the mouse tibia. The in vivo efficacy of the MTSS1 siRNA in silencing the endogenous mRNA expression was tested in mice 48 h after receiving intra-tibial transfection, with the mice receiving control siRNA as control. In brief, BMSCs were collected from the tibiae, cultured in complete α-MEM medium, then underwent RNA extraction and qRT-PCR to analyze the gene expression. To investigate the in vivo physiological role of MTSS1, the male mice aged 8 weeks were randomly allocated into 2 groups and received intratibial marrow transfection of either MTSS1 siRNA or control siRNA. The mice received the transfections twice in total, with an interval of 3 weeks. The mice were sacrificed 1 month after the 1st transfection and the tibia samples were collected and subjected to histomorphological and immunohistochemical analyses.

Histological staining and immunohistochemical staining

After dissection, the tibiae samples were processed for sectioning and histological analyses. Briefly, the samples were fixed with 10% neutral buffered formalin for 3 days, decalcified with 14% EDTA (pH 7.4) for 21 days, and embedded in paraffin. Sagittal sections were cut at 4 μm thick.

For the overall observation of the bone and detection of adipocytes in the marrow, the sections were stained with hematoxylin and eosin (H&E) following standard protocols. The quantity of the bone marrow fat was determined by measuring the numbers and areas of adipocytes on the sections. For the detection of osteoclasts, the sections were stained with tartrate-resistant acid phosphatase (TRAP) staining solution which consists of acetate buffer (0.1 M, pH 5.0), naphthol AS-MX phosphate (0.1 mg/ml), fast red violet LB salt (0.6 mg/mL), and sodium tartrate (0.05 M). Osteoclast numbers and surfaces were determined. For the detection of osteoblasts, the sections were subjected to immunohistochemical staining. In brief, the paraffin-embedded samples were deparaffinized in xylene, and rehydrated in decreasing concentrations of ethanol, then digested with 0.05% trypsin at 37 °C for 15 min for antigen retrieval. Endogenous peroxidases were quenched by incubation with 3% hydrogen peroxide for 15–20 min. Following blocking of non-specific binding with 1% BSA, the sections were probed overnight at 4 °C with primary anti-ALP (Abcam) or anti-phospho-Src antibody (Affinity), then incubated with HRP-conjugated secondary antibody. The immunoreaction was developed with the chromogen substrate 3,3′-diaminobenzidine (DAB) and the nuclei were counterstained with hematoxylin. The numbers of ALP- and phospho-Src-positive cells on the trabeculae were counted. The region of interest for the measurements starts from 0.1 mm below the growth plate and is 1 mm in length.

Statistical analysis

Data represent mean $\pm$ SD. Student's t test and ANOVA test were conducted for comparisons between two groups and multiple groups, respectively. One-way ANOVA was applied when there is only one independent variable and two-way ANOVA was applied when there are two independent variables. Tukey test was conducted for post hoc comparisons. A value of $p < 0.05$ was regarded as significant.

Availability of data and material The data that support the findings of this study are available from the corresponding author upon reasonable request.

Declarations

References

1. Chen Q, Shou P, Zheng C, Jiang M, Cao G, Yang Q, Cao J, Xie N, Velletri T, Zhang X et al (2016) Fate decision of mesenchymal stem cells: adipocytes or osteoblasts? Cell Death Differ 23:1128–1139

2. Veldhuis-Vlug AG, Rosen CJ (2017) Mechanisms of marrow adiposity and its implications for skeletal health. Metabolism 67:106–114

3. Wu M, Chen G, Li YP (2016) TGF-beta and BMP signaling in osteoblast, skeletal development, and bone formation, homeostasis and disease. Bone Res 4:16009

4. Nakashima K, Zhou X, Kunkel G, Zhang Z, Deng JM, Behringer RR, de Crombrugghe B (2002) The novel zinc finger-containing transcription factor osterix is required for osteoblast differentiation and bone formation. Cell 108:17–29

5. Alman BA (2015) The role of hedgehog signalling in skeletal health and disease. Nat Rev Rheumatol 11:552–560

6. Salazar VS, Gamer LW, Rosen V (2016) BMP signalling in skeletal development, disease and repair. Nat Rev Endocrinol 12:203–221

7. Lerner UH, Ohlsson C (2015) The WNT system: background and its role in bone. J Intern Med 277:630–649

8. Mota de Sa P, Richard AJ, Hang H, Stephens JM (2017) Transcriptional regulation of adipogenesis. Compr Physiol 7:635–674

9. Sadie-Van Gijsen H, Hough FS, Ferris WF (2013) Determinants of bone marrow adiposity: the modulation of peroxisome proliferator-activated receptor-gamma2 activity as a central mechanism. Bone 56:255–265

10. Xie F, Ye L, Ta M, Zhang L, Jiang WG (2011) MTSS1: a multifunctional protein and its role in cancer invasion and metastasis. Front Biosci (Schol Ed) 3:621–631

11. Lee YG, Macoska JA, Korenchuk S, Pienta KJ (2002) MIM, a potential metastasis suppressor gene in bladder cancer. Neoplasia 4:291–294

12. Du P, Wang S, Tang X, An C, Yang Y, Jiang WG (2017) Reduced expression of metastasis suppressor-1 (MTSS1) accelerates progression of human bladder Uroepithelium cell carcinoma. Anticancer Res 37:4499–4505

13. Du P, Ye L, Ruge F, Yang Y, Jiang WG (2011) Metastasis suppressor-1, MTSS1, acts as a putative tumour suppressor in human bladder cancer. Anticancer Res 31:3205–3212

14. Wang Y, Liu J, Smith E, Zhou K, Liao J, Yang GY, Tan M, Zhan X (2007) Downregulation of missing in metastasis gene (MIM) is associated with the progression of bladder transitional carcinomas. Cancer Invest 25:79–86

15. Yu J, Shen W, Gao B, Xu J, Gong B (2020) Metastasis suppressor 1 acts as a tumor suppressor by inhibiting epithelial-to-mesenchymal transition in triple-negative breast cancer. Int J Biol Markers 35:74–81

16. Zeleniak AE, Huang W, Fishel ML, Hill R (2018) PTEN-dependent stabilization of MTSS1 inhibits metastatic phenotype in pancreatic ductal adenocarcinoma. Neoplasia 20:12–24

17. Chen L, Chen Q, Wu Y, Zhu M, Hu J, Zhuang Z (2021) MTSS1 inhibits colorectal cancer metastasis by regulating the CXCR4/CXCL12 signaling axis. Int J Mol Med. https://doi.org/10.3892/ijmm.2021.4898

18. Wang H, Yu X, Wang X, Li X, Yang S (2017) Missing in metastasis B, regulated by DNMT1, functions as a putative cancer suppressor in human lung giant-cell carcinoma. Acta Biochim Biophys Sin 49:238–245

19. Mertz KD, Pathria G, Wagner C, Saarikangas J, Sboner A, Romanov J, Gschaider M, Lenz F, Neumann F, Schreiner W et al (2014) MTSS1 is a metastasis driver in a subset of human melanomas. Nat Commun 5:3465

20. Huang XY, Huang ZL, Xu B, Chen Z, Re TJ, Zheng Q, Tang ZY (2016) Elevated MTSS1 expression associated with metastasis and poor prognosis of residual hepatitis B-related hepatocellular carcinoma. J Exp Clin Cancer Res 35:85

21. Saarikangas J, Mattila PK, Varjosalo M, Bovellan M, Hakanen J, Calzada-Wack J, Tost M, Jennen L, Rathkolb B, Hans W et al (2011) Missing-in-metastasis MIM/MTSS1 promotes actin assembly at intercellular junctions and is required for integrity of kidney epithelia. J Cell Sci 124:1245–1255

22. Quinones GA, Jin J, Oro AE (2010) I-BAR protein antagonism of endocytosis mediates directional sensing during guided cell migration. J Cell Biol 189:353–367

23. Bershteyn M, Atwood SX, Woo WM, Li M, Oro AE (2010) MIM and cortactin antagonism regulates ciliogenesis and hedgehog signaling. Dev Cell 19:270–283

24. Brown AS, Meera P, Altindag B, Chopra R, Perkins EM, Paul S, Scoles DR, Tarapore E, Magri J, Huang H et al (2018) MTSS1/Src family kinase dysregulation underlies multiple inherited ataxias. Proc Natl Acad Sci U S A 115:E12407–E12416

25. Soriano P, Montgomery C, Geske R, Bradley A (1991) Targeted disruption of the c-src proto-oncogene leads to osteopetrosis in mice. Cell 64:693–702

26. Insogna KL, Sahni M, Grey AB, Tanaka S, Horne WC, Neff L, Mitnick M, Levy JB, Baron R (1997) Colony-stimulating factor-1 induces cytoskeletal reorganization and c-src-dependent tyrosine phosphorylation of selected cellular proteins in rodent osteoclasts. J Clin Invest 100:2476–2485

27. Boyce BF, Yoneda T, Lowe C, Soriano P, Mundy GR (1992) Requirement of pp60c-src expression for osteoclasts to form ruffled borders and resorb bone in mice. J Clin Invest 90:1622–1627

28. Marzia M, Sims NA, Voit S, Migliaccio S, Taranta A, Bernardini S, Faraggiana T, Yoneda T, Mundy GR, Boyce BF et al (2000) Decreased c-Src expression enhances osteoblast differentiation and bone formation. J Cell Biol 151:311–320

29. Haraguchi K, Nishida A, Ishidate T, Akiyama T (2004) Activation of beta-catenin-TCF-mediated transcription by non-receptor tyrosine kinase v-Src. Biochem Biophys Res Commun 313:841–844

30. Karni R, Gus Y, Dor Y, Meyuhas O, Levitzki A (2005) Active Src elevates the expression of beta-catenin by enhancement of cap-dependent translation. Mol Cell Biol 25:5031–5039

31. Yokoyama N, Malbon CC (2009) Dishevelled-2 docks and activates Src in a Wnt-dependent manner. J Cell Sci 122:4439–4451

32. Zhang QQ, Zhou DL, Lei Y, Zheng L, Chen SX, Gou HJ, Gu QL, He XD, Lan T, Qi CL et al (2015) Slit2/Robo1 signaling promotes

intestinal tumorigenesis through Src-mediated activation of the Wnt/beta-catenin pathway. Oncotarget 6:3123–3135

33. Condello S, Cao L, Matei D (2013) Tissue transglutaminase regulates beta-catenin signaling through a c-Src-dependent mechanism. FASEB J 27:3100–3112

34. Chen Q, Su Y, Wesslowski J, Hagemann AI, Ramialison M, Wittbrodt J, Scholpp S, Davidson G (2014) Tyrosine phosphorylation of LRP6 by Src and Fer inhibits Wnt/beta-catenin signalling. EMBO Rep 15:1254–1267